4D-CTA in Neurovascular Disease: A Review

H.G.J. Kortman, E.J. Smit, M.T.H. Oei, R. Manniesing, M. Prokop, and F.J.A. Meijer

ABSTRACT

SUMMARY: CT angiography is a widely used technique for the noninvasive evaluation of neurovascular pathology. Because CTA is a snapshot of arterial contrast enhancement, information on flow dynamics is limited. Dynamic CTA techniques, also referred to as 4D-CTA, have become available for clinical practice in recent years. This article provides a description of 4D-CTA techniques and a review of the available literature on the application of 4D-CTA for the evaluation of intracranial vascular malformations and hemorrhagic and ischemic stroke. Most of the research performed to date consists of observational cohort studies or descriptive case series. These studies show that intracranial vascular malformations can be adequately depicted and classified by 4D-CTA, with DSA as the reference standard. In ischemic stroke, 4D-CTA better estimates thrombus burden and the presence of collateral vessels than conventional CTA. In intracranial hemorrhage, 4D-CTA improves the detection of the "spot" sign, which represents active ongoing bleeding.

ABBREVIATIONS: dAVF = dural arteriovenous fistula; TI-CTA = timing-invariant CTA

Multidetector row CT angiography has enabled rapid noninvasive evaluation of the intracranial vasculature for acute neurologic conditions such as subarachnoid hemorrhage or ischemic stroke. While the anatomic evaluation is excellent, the evaluation of flow dynamics is limited with CTA because information is obtained from only 1 single time point during the passage of a contrast bolus.[1,2]

Diagnostic catheter-based digital subtraction angiography has been widely replaced by CTA as a diagnostic procedure but retains its value if very high spatial resolution is required or the flow dynamics of a cerebral vascular abnormality need to be assessed. Remaining indications for DSA include work-up of vascular malformations or the evaluation of collateral vessels in obstructive arterial disease. In addition, DSA is considered the criterion standard for the detection of aneurysms in nontraumatic subarachnoid hemorrhage. Drawbacks of DSA are the relatively time-consuming procedure, high cost, radiation exposure for both patient and operator,[3,4] a low but nonnegligible risk of transient or permanent neurologic complications,[5-7] and an even higher risk of silent embolic events.[8]

From the Department of Radiology and Nuclear Medicine, Radboud University Nijmegen Medical Center, Nijmegen, the Netherlands.

Please address correspondence to Frederick J.A. Meijer, MD, Geert Grooteplein 10, 6500 HB Nijmegen, the Netherlands; e-mail: Anton.Meijer@radboudumc.nl

Indicates open access to non-subscribers at www.ajnr.org

Indicates article with supplemental on-line table.

Indicates article with supplemental on-line video.

http://dx.doi.org/10.3174/ajnr.A4162

Dynamic CTA has been developed in recent years as a technique that combines the noninvasive nature of CTA with the dynamic acquisition of DSA. The technique is also referred to as 4D-CTA and enables the noninvasive evaluation of flow dynamics of the intracranial vasculature by multiple subsequent CT acquisitions or a continuous volume CT acquisition for a period of time.

The value of 4D-CTA compared with CTA and DSA has been the subject of an increasing number of publications within the past decade. This article provides a description of the 4D-CTA techniques and reviews the current literature on the application of cranial 4D-CTA in hemorrhagic and ischemic stroke and the evaluation of intracranial arteriovenous malformations and arteriovenous fistulas.

Imaging Technique

Data Acquisition. Various approaches have been developed to provide whole-brain coverage of 4D-CTA: a toggling-table technique, shuttle mode scanning, or volume mode (Fig 1). The width of the CT detector determines which acquisition mode can be used to ensure coverage of the whole brain.

The most versatile option is a volume mode, which allows complete or partial coverage of the whole brain during 1 rotation. Detector configurations that cover the whole brain with 16-cm coverage are now available from 2 major vendors and have been implemented as 320 × 0.5 mm or 256 × 0.625 mm collimations. Scanners with 4- to 8-cm coverage acquire smaller portions of the cerebral vascular system, usually including the region of the circle of Willis and above.[9]

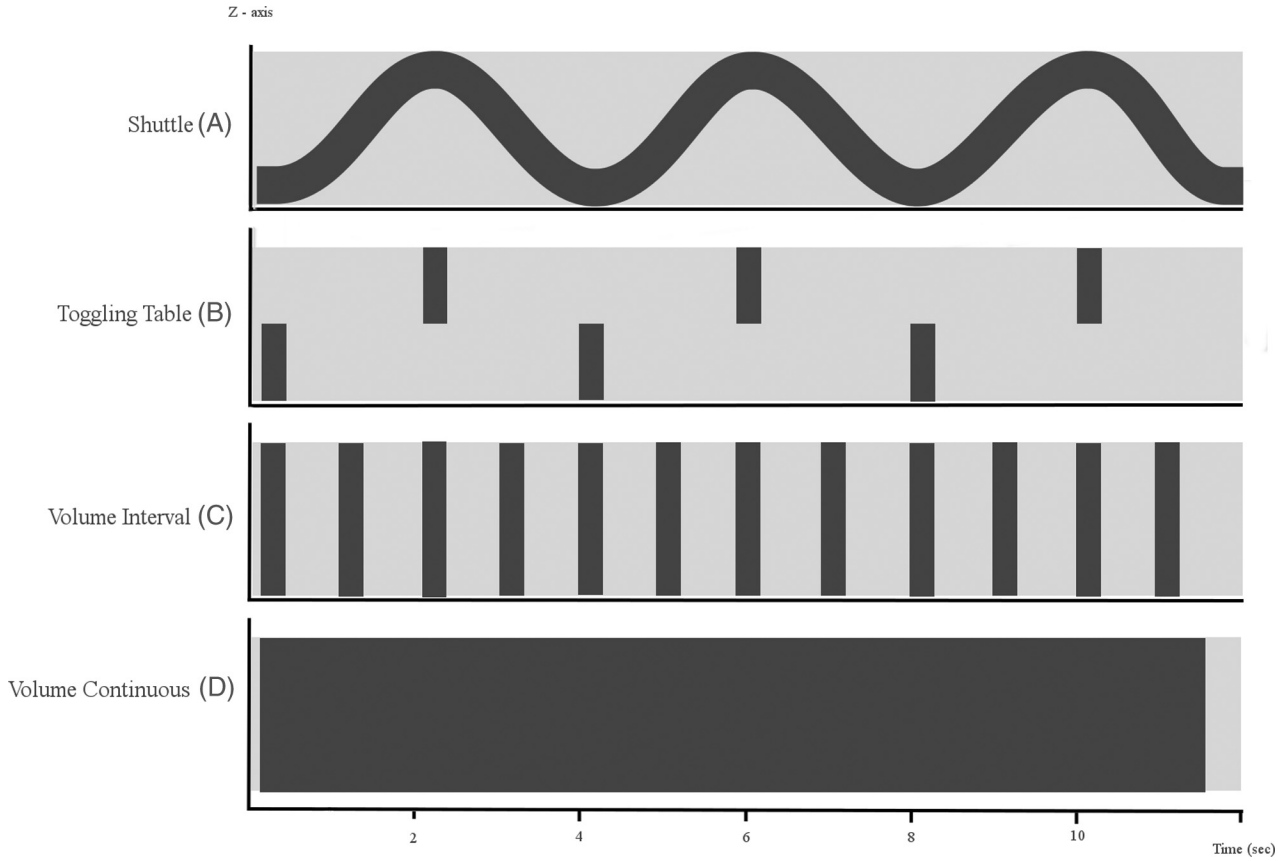

FIG 1. Schematic diagram of 4D-CTA imaging techniques. The x-axis represents the time domain. The y-axis represents the z-dimension. The light-gray horizontal bar represents the area that needs to be covered in the z-dimension. *A*, Shuttle mode: the sinus represents continuous table movement back and forth in the z-axis dimension to provide adequate coverage of the region of interest at multiple points in time. Notice that the temporal resolution is a function of the speed of table movement, typically 2–4 seconds depending on coverage. *B*, Toggling-table technique: the bars represent table repositioning in the z-axis dimension to provide adequate coverage of the region of interest at multiple points in time. Notice that the temporal resolution is a function of the speed of table repositioning, typically 3–4 seconds. *C*, Volume scanning: complete coverage of the region of interest (horizontal bar) with 1 gantry rotation. Notice that the temporal resolution is a function of the scanning interval settings because each rotation provides full coverage. Volume CT scanning enables (*D*) continuous volume scanning. Temporal resolution is limited by the gantry rotation speed.

Dynamic acquisitions with this volume mode can be performed discontinuously or continuously, depending on the required temporal resolution. The sequence of 3D datasets acquired with the discontinuous acquisition mode is sampled according to preset fixed or variable temporal intervals, usually in the range of 1- to 4-seconds. True 4D-datasets from the continuous scanning mode are acquired continuously during a period of time. These continuously acquired data can then be retrospectively reconstructed at any time interval. While the reconstructed time interval can be as little as 20 ms, the data for each reconstructed 3D volume are sampled during one-half to 1 gantry rotation, usually on the order of 0.275–0.5 seconds. In the case of continuous volume acquisitions and narrow temporal reconstruction intervals, the reconstructed data overlap in the temporal domain, very similar to overlapping data created from helical scanning in the spatial domain.[10] Continuous scanning is possible only in volume mode.

The toggling-table technique increases coverage by continuously switching between adjacent regions with fast table movement.[11] The minimum time intervals between subsequent acquisitions of each of the 2 regions is limited by the detector width and the speed of table movement. The temporal resolution typically allows a scan interval in the range of 2–4 seconds.[12] One has to be aware, however, that the enhancement curve of the cerebral vasculature is sampled differently for both scan regions, with an interleaving sampling pattern. Artifacts at the interface between regions may arise because enhancement differs between consecutive scans; this difference could impair the evaluation of flow dynamics or the detection of steno-occlusive vessel disease. A detector width of approximately 8 cm is required to image the entire brain in 2 acquisitions. For scanners with smaller detector widths, shuttle mode scanning is preferred to obtain whole-brain coverage because the temporal resolution will be significantly reduced with the toggling-table technique.

In shuttle mode scanning, a continuous helical acquisition is performed while the table moves smoothly to and fro to cover the desired scan range. This is the preferred mode for all scanners that cannot cover the whole area within 1 volume. Compared with the toggling-table technique, the shuttle mode is more flexible with regard to the length of coverage and does not create artifacts at the border between adjacent regions. However, temporal sampling intervals are only constant for the center of the scan range. Further to the periphery of the scan range, sampling intervals alternate between progressively shorter and longer periods (Fig 1).

Radiation Dose. The cumulative dose of 4D-CTA is the sum of the radiation doses of the individual acquisitions. Even if each of these acquisitions uses a lower dose than conventional CTA, the cumulative dose of 4D-CTA is usually substantially higher than that in conventional CTA.[13,14] Reducing the dose of individual acquisitions further will lead to excessive image noise. This needs to be counterbalanced by image filtering or iterative reconstruction. Proper image filtering will allow substantial dose reduction with preservation of or even increase in diagnostic image quality.[15,16] The use of iterative reconstructions has enabled a radiation-dose reduction with preserved image quality.[17]

The radiation dose becomes larger as the number of acquisitions during 4D-CTA or the dose per acquisition is increased. Continuous scanning delivers the highest dose. A faster gantry rotation time at identical milliampere-second settings will reduce the dose but increase the noise. The cumulative milliampere-second values are a good relative indicator of radiation exposure. At a setting of 200 mAs and a rotation time of 0.275 ms, each rotation delivers 55 mA. If for 40 seconds, an acquisition is performed every 2 seconds for a total of 20 acquisitions, the cumulative exposure becomes 55 mA $\times$ 20 = 1100 mA, which is identical to a continuous acquisition of 5.5 seconds (5.5 seconds $\times$ 200 mA = 1100 mAs).

Comparison of the radiation dose between CTA and DSA is challenging because of different geometries of the x-ray beam. In addition, radiation exposure is reported by using different units of measurement.[18] An effective radiation dose, however, can be compared but varies greatly depending on the scanning technique for 4D-CTA and the complexity of the procedure and the number of contrast runs during DSA. Effective doses of 5–6 mSv have been reported for 4D-CTA and 2–4.5 mSv for diagnostic cerebral DSA.[3,18,19] Doses reported for therapeutic interventions are substantially higher. Skin doses of >10,000 mGy may be accumulated during complex procedures.[20,21]

Image Processing. 4D-CTA generates a large amount of data that depends on the number of reconstructed 3D volumes and the reconstruction increment of each 3D volume. For example, a shuttle acquisition that covers 150 mm and uses 10 passes to and fro creates 2 $\times$ 10 datasets. If each dataset is reconstructed as a 1-mm section with a 1-mm increment, the total number of CT images is 20 $\times$ 150 = 3000. If overlapping reconstruction with a 0.5-mm increment is used, the number of images doubles to 6000. A discontinuous volume acquisition consisting of 20 scans with 320 $\times$ 0.5 mm detector collimation reconstructed as 0.5-mm sections with a 0.5-mm increment will create 320 $\times$ 20 = 6400 images. If the increment is reduced to 0.25 mm, which provides high-quality isotropic imaging, the number doubles to 12,800 images. A continuous-volume CT acquisition with 320 $\times$ 0.5 mm collimation during 10 seconds reconstructed at a frame rate of 10 per second and 0.5-mm increments results in 320 $\times$ 10 $\times$ 10 = 32,000 images. These numbers increase when additional image planes are reconstructed.

This huge number of images requires powerful workstations and optimized data postprocessing. Viewing the data as thin sections is possible but very ineffective, given the total number of images to be reviewed. This mode is reserved for problem solving.

Maximum intensity projections provide a much better overview of the vasculature and are the standard mode of viewing 4D data. Because of superimposing bone, usually thin slabs of 10–20 mm are viewed interactively. Small vascular structures are better evaluated in multiplanar reconstructions.

Alternatively, bone subtraction can be performed. The various 3D datasets should be aligned by rigid or nonrigid registration to compensate for patient motion during the 4D acquisition. If a patient moves during an acquisition, the dataset becomes slightly distorted and rigid registration leads to artifacts in the moving areas. These problems can be avoided by nonrigid approaches.

Bone subtraction then can be performed by subtracting the nonenhanced scan from each subsequent acquisition. This procedure, however, substantially increases image noise. Therefore, bone masking is frequently performed. This technique identifies bones as high-attenuation objects on the nonenhanced scan and removes these from the subsequent contrast-enhanced 4D sequence (On-line Videos).

MIP of these bone-subtracted data creates DSA-like images that can be viewed as a temporal sequence that shows contrast inflow and washout. As an alternative to MIP, volume-rendering, which provides more morphologic detail of the vessel lumen, can be performed.

The vascular morphology can best be evaluated if the whole 4D dataset is condensed into a 3D dataset by using temporal MIP, which displays the brightest voxel across all time points. If one filters the data in the temporal domain, spatial resolution remains intact while image noise is reduced and image quality is substantially improved. The resulting so-called timing-invariant CTA (TI-CTA) creates a high-quality timing-insensitive MIP of the vascular tree.[22]

Several studies reported inferior or comparable image quality of 4D-CTA and conventional CTA.[13,14,19] TI-CTA, on the other hand, was shown to have a 43% higher contrast-to-noise ratio and a 28% lower image noise compared with conventional CTA.[16] In addition, TI-CTA was rated as having less vascular noise, better vascular contour, better detail visibility of medium arteries, better detail visibility of small arteries, and better overall image quality than conventional CTA and 4D-CTA.[16]

Choice of Acquisition Technique. The choice between a continuous or noncontinuous 4D-CTA acquisition depends on the available scanning modes and is limited to noncontinuous acquisitions in case of toggling-table or shuttle modes. In patients suspected of having a high-flow vascular malformation, such as a dural AVF (dAVF) or AVM, the detection of abnormal early filling of venous structures requires a high temporal resolution of 4D-CTA. These cases profit from continuous acquisition (Fig 2). When collateral flow in case of an arterial occlusion needs to be evaluated, a lower temporal resolution will be sufficient.

Review of Literature on 4D-CTA in Neurovascular Disease

Vascular Malformations. An arteriovenous malformation is an abnormal communication between an artery and a vein with a network of abnormal intervening vessels, referred to as a nidus. An arteriovenous fistula is an abnormal communication between an artery and a venous structure without a nidus. For planning endovascular or surgical treatment, various grading systems have

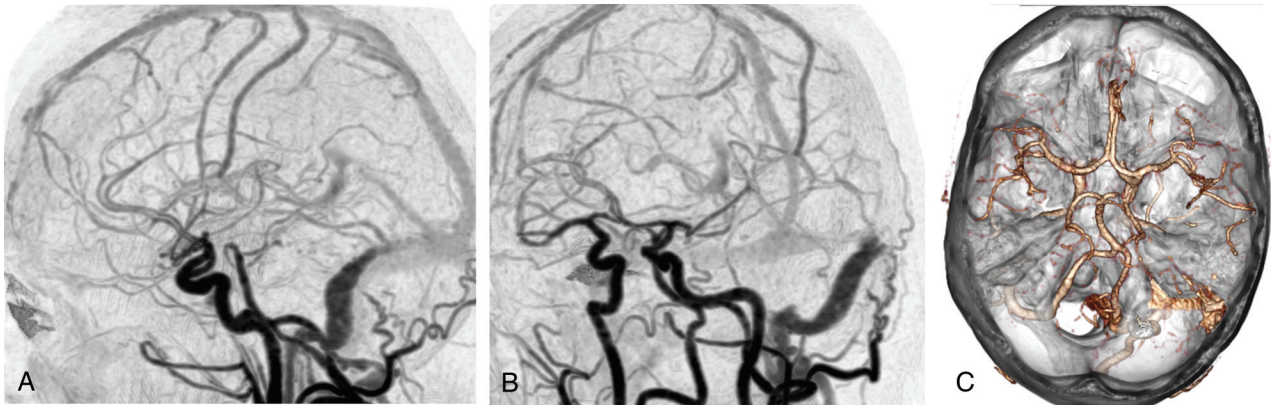

FIG 2. 4D-CTA demonstrating a Borden type I dural arteriovenous fistula of the left sigmoid sinus. Selected 4D-CTA subtraction MIP images of a continuous 4D-CTA volume acquisition (320–detector row CT) in lateral (*A*) and oblique (*B*) projections in a patient presenting with left-sided tinnitus. Branches of the occipital artery are identified as arterial feeders of the dAVF. There is normal antegrade venous return. The 3D image (*C*) demonstrates the advantage of 4D-CTA to study vessels in relation to surrounding structures.

Classification of arteriovenous malformations and arteriovenous fistulas

Pathology	AVM	AVF
Distinguishing feature	Presence of a nidus	No nidus
Grading system	Spetzler-Martin classification	Cognard classification
		Borden classification
Classification	Spetzler-Martin AVM grading scale	Cognard classification:
	Size	Grade I: in sinus wall; normal antegrade venous drainage
	Small (<3 cm) = 1	Grade IIa: in sinus; reflux to sinus, not cortical veins
	Medium (3–6 cm) = 2	Grade IIb: retrograde drainage (reflux) to cortical veins
	Large (>6 cm) = 3	Grade III: direct cortical venous drainage; no venous ectasia
	Eloquence of adjacent brain	Grade IV: direct cortical venous drainage and venous ectasia
	Noneloquent = 0	Grade V: Spinal perimedullary venous drainage
	Eloquent = 1	Borden classification:
	Venous drainage	Type I: dural arterial supply with antegrade venous drainage
	Superficial only = 0	Type Ia: simple dAVF with single meningeal arterial supply
	Deep component = 1	Type Ib: complex dAVF with multiple meningeal arteries
		Type II: retrograde cortical venous drainage
		Type III: dural arteries drain into cortical veins

been developed on the basis of imaging characteristics. Features include the location of the lesion, presence and size of a nidus, number and size of the feeding arteries, and the patterns of venous drainage (Table). The most commonly used grading system for AVMs is the Spetzler-Martin system.[23] The Cognard classification and Borden classification are most commonly used for dAVFs.[24,25] These classification systems were originally developed on the basis of DSA but can also be applied to 4D-CTA.

Adequate depiction of the angioarchitectural features of intracranial vascular malformations is essential for hemorrhage risk assessment and treatment planning.[23-25] The high temporal and spatial resolution required could, until recently, only be provided by DSA. Studies that compare 4D-CTA with DSA for the evaluation of brain AVMs and AVFs include descriptive case series and observational cohort studies (On-line Table). Because none of these exceed level 3 evidence, further research is warranted to assess the role of 4D-CTA in the work-up of craniospinal vascular malformations.

Wang et al[26] compared 4D-CTA and DSA examinations for diagnosing AVMs in 17 patients. They found that 4D-CTA was consistent with DSA in all cases for AVM location, size, and vascular structures. Compared with DSA, 4D-CTA could distinguish the main feeding arteries and successfully identify all draining veins in all patients. In 1/17 patients, however, there were discrepancies in the identification of smaller and specific arterial branches. Good correlation of 4D-CTA with DSA for the detection and grading of cerebral AVMs was also found by Willems et al.[27] In 17 patients, all AVMs were detected by 4D-CTA. With regard to the Spetzler-Martin grade, 4D-CTA disagreed with DSA in 1 patient in whom deep venous drainage was missed.

In a study comparing 4D-CTA and DSA in patients with a variety of cerebrovascular pathology, physiologic and abnormally shortened cerebral circulation times were comparable for 4D-CTA and DSA.[28]

Abnormal venous drainage is the hallmark of classifying a dAVF. Retrograde venous flow in cortical veins, which is associated with increased risk of hemorrhage,[24] can be visualized by using 4D-CTA.[24] Performance of 4D-CTA was similar to that of DSA for the diagnosis and grading of dAVFs. Fujiwara et al[29] compared 4D-CTA with DSA in 29 patients for diagnosis, classification, and follow-up of dAVFs. DSA depicted 33 dAVFs in 28 cases (in 1 subject the dAVF was resolved after endovascular treatment). By consensus reading, 4D-CTA correctly detected 32/33 dAVFs in 27 cases and properly graded 31/33 lesions by using the Cognard classification.[24] Spinal venous drainage was missed by both readers on 4D-CTA in a case with a Cognard type V dAVF. In 1 case, 1 reader missed cortical venous reflux on 4D-CTA.

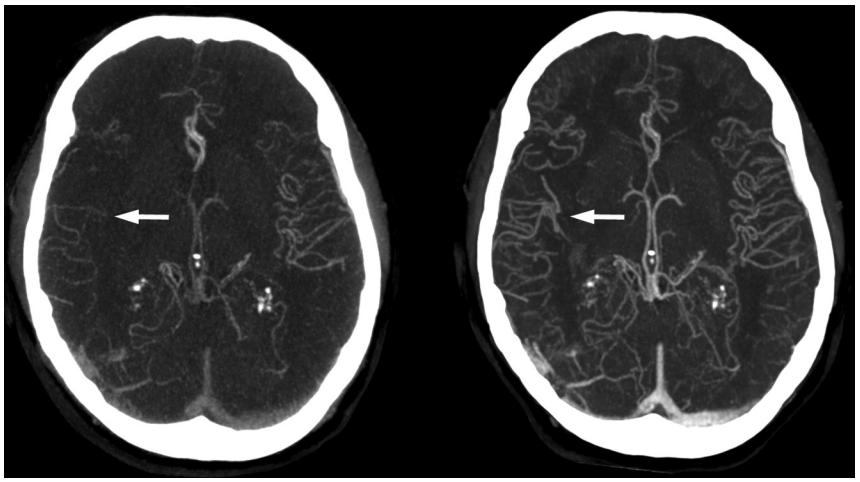

FIG 3. Timing-invariant CTA better estimates the extent of collateral circulation in a patient with right middle cerebral artery occlusion. The *left* image is a conventional CTA showing poor collateral circulation and suggests a poor prognosis. The *right* image is a TI-CTA image from a 4D-CTA acquisition (ie, temporal MIP), which shows good collateral filling and suggests a good prognosis. In this case, the patient had a good recovery.

Intermodality agreement for the presence and classification of dAVFs was excellent ($\kappa = 0.955$ and 0.921, respectively). 4D-CTA detected 77 of 109 feeding arteries (71%) in 25 cases. In 3 cases with a dAVF located at the cavernous sinus, neither reader could detect any feeding arteries. The intermodality agreement for the number of feeding arteries of dAVFs was good ($\kappa = 0.713$). Prior studies support the accuracy of 4D-CTA for the diagnosis and classification of dAVFs with DSA as the reference standard.[30-33]

A single report evaluated spinal dAVFs and compared 4D-CTA with MRA and DSA.[34] 4D-CTA could detect the perimedullary veins and the location of the AVF in 3/4 cases. The direction of venous flow was correctly assessed in all cases. The authors, however, used a high-dose technique in the thoracolumbar region with a reported effective dose of >40 mSv. Because the evaluation of the spine for the detection of a vascular malformation requires coverage of a large area, the use of 4D-CTA as a first screening tool is probably limited. Thus, 4D-MRA has the advantage of extended coverage and lack of radiation exposure.

Hemorrhagic Stroke. In patients with intracranial hemorrhage, CTA is used to evaluate potential underlying neurovascular pathology such as aneurysms or vascular malformations. Another application is to detect extravasation of contrast material, also termed the "spot" sign. The spot sign is associated with hematoma expansion and increased mortality.[35,36] In a prospective evaluation, Sun et al[37] found the spot sign to be present throughout the arterial-to-venous phases on 4D-CTA studies of 112 patients and it was an independent predictor of hematoma progression. In comparison with conventional CTA, the spot sign on 4D-CTA had a higher predictive value for hematoma expansion; therefore, 4D-CTA seems to be more accurate for estimating prognosis. The false-negative results of CTA can be explained by the time it takes for contrast extravasation to manifest, so the single acquisition of conventional CTA may be too early.

Ischemic Stroke. In the work-up of patients presenting with ischemic stroke, 4D-CTA demonstrated added value over conventional CTA for the evaluation of the extent and dynamics of collateral flow.[38]

The length and location of the thrombus burden in case of intracranial vessel occlusion have been used to predict therapy response, with larger proximal thrombus considered more resistant to intravenous thrombolytic therapy.[39] Frölich et al[40] found better demarcation of thrombus burden in patients with anterior circulation occlusion by using 4D-CTA compared with conventional CTA due to better visualization of collateral circulation.

For endovascular procedures, the angiographic appearance of the occlusion site has been used as a predictor of recanalization success.[41,42] In particular, angiographic demonstration of delayed antegrade contrast opacification distal to the occlusion site referred to as the "clot outline" sign has been linked to improved recanalization rates after intra-arterial thrombolytic therapy.[43] 4D-CTA has been comparable with DSA in discriminating antegrade and retrograde flow across a cerebral artery occlusion.[44] The presence of antegrade flow on 4D-CTA is associated with an increased chance of early vessel recanalization by using intravenous thrombolysis.[44]

The extent of infarcted brain tissue generally depends on the location of the vessel occlusion and the time to recanalization.[45] In recent years, it has become clear that the extent of collateral circulation is an important independent factor for the extent of infarction and clinical outcome.[46] Collateral blood flow is also an independent prognostic factor for successful thrombolytic therapy.[47,48] In accordance with these findings, collateral grading on CTA has been shown to be a strong and independent prognostic factor for clinical outcome after acute stroke.[49] In particular, the absence of leptomeningeal collaterals has been shown to be highly predictive for poor clinical outcome.[50] However, the absence of collaterals on conventional CTA may not be a correct representation of true collateral blood supply: The acquisition may be too early to display collaterals with delayed filling.[38] Absence of collaterals on 4D-CTA should be a better measure because delayed enhancement can be captured during the acquisition sequence. As a result, 4D-CTA should also be a stronger predictor of patient outcome after stroke.[51] In a prospective cohort study in 40 subjects, Smit et al[22] compared CTA with TI-CTA calculated from 4D-CTA data in patients presenting with ischemic stroke. Patients with poor collateral circulation on conventional CTA were still found to have good clinical outcome in 31% of cases. On TI-CTA, this subgroup of patients was found to have good collaterals (Fig 3). Conversely, all patients with poor collateral status on TI-CTA also showed poor clinical outcome. Another recent study supports these findings.[40]

Whole-brain perfusion maps can be calculated from 4D-CTA data, which enables the correlation between parenchyma perfusion deficits and the detection of vessel occlusions.[52]

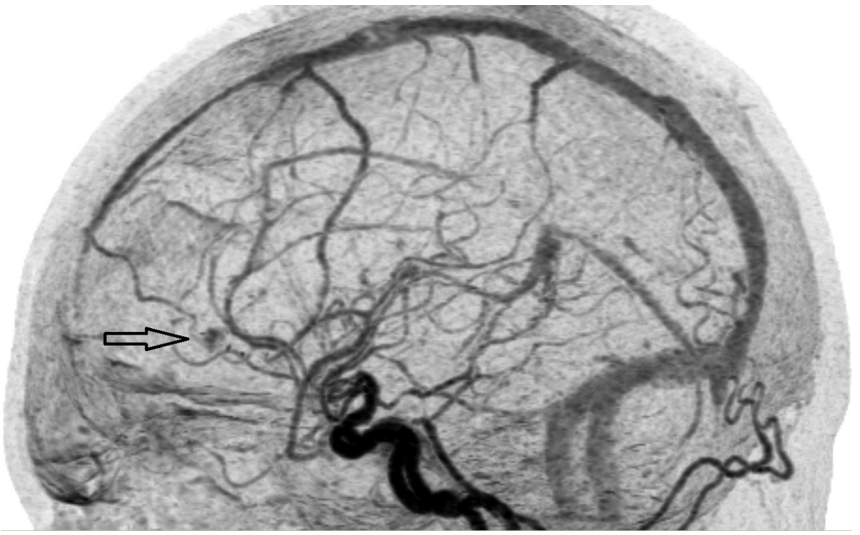

FIG 4. 4D-CTA image demonstrating recurrence of an arteriovenous malformation. The *arrow* indicates the nidus, which is fed by arterial feeders from the anterior cerebral artery. There is cortical venous drainage toward the rostral superior sagittal sinus.

Chronic Arterial Disease. In case of proximal vascular stenotic or occlusive disease, 4D-CTA can be used to study altered flow dynamics of the intracranial vasculature, for example, to evaluate collateral flow via the circle of Willis. In a retrospective study with 25 patients with proximal vessel occlusion, Menon et al[53] could differentiate distinct patterns of collaterals. These patterns consisted of posterior cerebral artery–MCA dominant collateralization, intratentorial leptomeningeal collaterals, and variability in size, extent, and retrograde filling time in pial arteries.

Discussion

4D-CTA has enabled noninvasive evaluation of flow dynamics of neurovascular pathology. High temporal resolution for the detection and classification of intracranial AVMs and AVFs can be achieved by a continuous volume acquisition, though for whole-brain coverage, a wide detector is required. In case of smaller detector width, the toggling-table technique or shuttle mode scanning enables 4D-CTA with extended coverage in which a lower temporal resolution seems to be acceptable for the evaluation of ischemic or hemorrhagic stroke. The main challenge for routine clinical use of 4D-CTA is to keep the radiation dose at bay, which strongly depends on the acquisition parameters used. Because dose-reduction techniques such as iterative reconstruction and noise-reduction filters already have reduced the radiation dose dramatically, the challenge now is to bring the radiation dose of 4D-CTA down to the level of conventional CTA so that the clinical application can be extended. To achieve consistent high image quality, image registration and filtering techniques should be further improved. This change can result in better depiction of small, clinically important vascular structures on 4D-CTA. DSA is still superior to 4D-CTA with respect to spatial resolution and the possibility of selective vessel contrast injection.

Future Perspectives and Clinical Implementation. Detection of the main arterial feeders and patterns of venous drainage by 4D-CTA seems to be sufficient in most cases to correctly identify and classify brain AVMs and AVFs. This can be used for treatment planning, which would save the patient a preinterventional invasive DSA. In addition, 4D-CTA could replace an invasive DSA in the follow-up of intracranial vascular malformations (Fig 4). The advantage of a noninvasive procedure is evident, and the decrease in spatial resolution does not seem to change clinical management for most patients. However, this needs to be addressed in larger cohort studies. In ischemic stroke, 4D-CTA or timing-invariant CTA displays the presence and extent of collateral vessels and thrombus burden more reliably than conventional CTA. This difference has important implications for prognosis assessment and treatment decision-making. The spot sign in intracranial hemorrhage is an indicator of acute contrast extravasation and is better detected by 4D-CTA than by conventional CTA. It is an independent predictor of outcome that may guide early surgical or endovascular treatment.

Currently, whole-brain coverage can be achieved with different dynamic CT techniques. However, additional evaluation of the cervical vessels is commonly necessary in the diagnostic work-up of stroke. An additional CTA of the neck would result in an additional contrast bolus and radiation exposure with already opacified venous structures as a result of the first contrast bolus. With the use of a wide detector, a volume neck CTA acquisition combined with dynamic volume acquisitions of the head is technically feasible,[54] though clinical application of this technique needs to be further evaluated.

CONCLUSIONS

There is increasing evidence that 4D-CTA has added value over conventional CTA for the diagnosis, treatment planning, and follow-up of different neurovascular disorders because 4D-CTA enables evaluation of flow dynamics. However, because level 3 evidence is mainly available, additional prospective clinical cohort studies are necessary, taking the scanning technique used into account. In addition, the radiation dose of 4D-CTA should be further reduced by improved filtering and registration techniques. Improved filtering and registration should result in improved image quality with better depiction of small vascular structures.

Appendix: Search Strategy

Methods. A systematic search was performed in the following data bases: MEDLINE by using PubMed, Cochrane Central Register of Controlled Trials, Web of Science (formerly ISI Web of Knowledge), and EMBASE via OvidSP. During the search, no restrictions were made with regard to language or date of publication. Reference and citation tracking of selected articles were included in the search. All abstracts were read, and relevant articles were selected.

Search. ("Stroke" [Medical Subject Headings or MeSH] OR "Intracranial Arteriovenous Malformations" [MeSH] OR "Central Nervous System Vascular Malformations" [MeSH] OR "Arteriovenous Fistula" [MeSH] OR "Subarachnoid Hemorrhage" [MeSH] OR "Aneurysm, Intracranial Berry, 1" [Supplementary Concept] OR Arteriovenous Malformation* [tiab] OR AVM* [tiab] OR AVF* [tiab] OR dAVF* OR Subarachnoid Hemorrhage* [tiab] OR Subarachnoid Bleed* [tiab] OR SAH* [tiab] OR SAB [tiab] OR SABs [tiab] OR Aneurysm* [tiab] OR Vascular Malformation* [tiab] OR Vascular Anomal* [tiab] OR Arteriovenous Fistula* [tiab] OR CVA* [tiab] OR Cerebrovascular [tiab] OR Neurovascular [tiab] OR Stroke* [tiab] OR Intracranial collateral* [tiab] OR Leptomeningeal collateral* OR Moyamoya [tiab]

OR

"Angiography, Digital Subtraction" [MeSH] OR Digital Subtraction Angiograph* [tiab] OR DSA [tiab] OR Subtraction Angiograph* [tiab] OR Cerebral Angiograph* [tiab] OR Spinal Angiograph* [tiab] OR cerebral angiograph* [tiab] OR "Cerebral Angiography" [MeSH])

AND

(Four Dimensional Computed Tomograph* [tiab] OR Whole brain CT* [tiab] OR Dynamic angiograph* [tiab] OR 4D Computed Tomograph* [tiab] OR 4D CT [tiab] OR Four Dimensional CAT [tiab] OR Four Dimensional CATs [tiab] OR Four Dimensional CT* [tiab] OR 4D CAT [tiab] OR 4D CATs [tiab] OR 4D CT* [tiab] OR 4DCT* [tiab] OR Time resolved 3D [tiab] OR Time resolved 4D [tiab] OR Dynamic 3D [tiab] OR Dynamic three dimensional [tiab] OR Dynamic CT* [tiab] OR Time resolved CT* [tiab] Or Time invariant CT* [tiab] OR Timing invariant CT* [tiab] OR "Four-Dimensional Computed Tomography "[MeSH]).

Results. We retrieved 328 articles.

Two reviewer authors independently selected the articles from the list of identified references. Consensus was sought, but when no consensus could be reached, a third review author was consulted. If relevance could not be ascertained on the basis of the abstract, the complete article was reviewed. The final decision of inclusion was then made on review of the full text.

Disclosures: Ewoud J. Smit—*UNRELATED*: *Payment for Lectures (including service on Speakers Bureaus)*: Toshiba Medical Systems (Speakers Bureau). Rashindra Manniesing—*RELATED*: *Grant*: Toshiba Medical Systems*; *UNRELATED*: *Grants/Grants Pending*: Dutch Technology Foundation (STW).* Mathias Prokop—*RELATED*: *Grant*: Philips Healthcare*; *UNRELATED*: *Grants/Grants Pending*: Philips Healthcare,* Toshiba Medical Systems*; *Payment for Lectures (including service on Speakers Bureaus)*: Bracco, Toshiba Medical Systems, Bayer-Schering, CME Science; *Travel/Accommodations/Meeting Expenses Unrelated to Activities Listed*: Toshiba Medical Systems, Philips Healthcare, European School of Radiology, CME Science. Frederick J.A. Meijer—*UNRELATED*: *Payment for Lectures (including service on Speakers Bureaus)*: Toshiba Medical Systems (Speakers Bureau). *Money paid to the institution.

REFERENCES

1. Klingebiel R, Siebert E, Diekmann S, et al. **4-D imaging in cerebrovascular disorders by using 320-slice CT: feasibility and preliminary clinical experience.** *Acad Radiol* 2009;16:123–29
2. Schellinger PD, Richter G, Kohrmann M, et al. **Noninvasive angiography (magnetic resonance and computed tomography) in the diagnosis of ischemic cerebrovascular disease: techniques and clinical applications.** *Cerebrovasc Dis* 2007;24(suppl 1):16–23
3. Alexander MD, Oliff MC, Olorunsola OG, et al. **Patient radiation exposure during diagnostic and therapeutic interventional neuroradiology procedures.** *J Neurointerv Surg* 2010;2:6–10
4. James RF, Wainwright KJ, Kanaan HA, et al. **Analysis of occupational radiation exposure during cerebral angiography utilizing a new real time radiation dose monitoring system.** *J Neurointerv Surg* 2014 May 14. [Epub ahead of print]
5. Willinsky RA, Taylor SM, terBrugge K, et al. **Neurologic complications of cerebral angiography: prospective analysis of 2,899 procedures and review of the literature.** *Radiology* 2003;227:522–28
6. Cloft HJ, Joseph GJ, Dion JE. **Risk of cerebral angiography in patients with subarachnoid hemorrhage, cerebral aneurysm, and arteriovenous malformation: a meta-analysis.** *Stroke* 1999;30:317–20
7. Kaufmann TJ, Huston J, Mandrekar JN, et al. **Complications of diagnostic cerebral angiography: evaluation of 19,826 consecutive patients.** *Radiology* 2007;243:812–19
8. Bendszus M, Koltzenburg M, Burger R, et al. **Silent embolism in diagnostic cerebral angiography and neurointerventional procedures: a prospective study.** *Lancet* 1999;354:1594–97
9. Morhard D, Wirth CD, Fesl G, et al. **Advantages of extended brain perfusion computed tomography: 9.6 cm coverage with time resolved computed tomography-angiography in comparison to standard stroke-computed tomography.** *Invest Radiol* 2010;45:363–69
10. Hoogenboom TC, van Beurden RM, van Teylingen B, et al. **Optimization of the reconstruction interval in neurovascular 4D-CTA imaging: a technical note.** *Interv Neuroradiol* 2012;18:377–79
11. Roberts HC, Roberts TP, Smith WS, et al. **Multisection dynamic CT perfusion for acute cerebral ischemia: the "toggling-table" technique.** *AJNR Am J Neuroradiol* 2001;22:1077–80
12. Youn SW, Kim JH, Weon YC, et al. **Perfusion CT of the brain using 40-mm-wide detector and toggling table technique for initial imaging of acute stroke.** *AJR Am J Roentgenol* 2008;191:W120–26
13. Saake M, Goelitz P, Struffert T, et al. **Comparison of conventional CTA and volume perfusion CTA in evaluation of cerebral arterial vasculature in acute stroke.** *AJNR Am J Neuroradiol* 2012;33:2068–73
14. Yang CY, Chen YF, Lee CW, et al. **Multiphase CT angiography versus single-phase CT angiography: comparison of image quality and radiation dose.** *AJNR Am J Neuroradiol* 2008;29:1288–95
15. Mendrik AM, Vonken EJ, van Ginneken B, et al. **TIPS bilateral noise reduction in 4D CT perfusion scans produces high-quality cerebral blood flow maps.** *Phys Med Biol* 2011;56:3857–72
16. Smit EJ, Vonken EJ, van der Schaaf IC, et al. **Timing-invariant reconstruction for deriving high-quality CT angiographic data from cerebral CT perfusion data.** *Radiology* 2012;263:216–25
17. Lin CJ, Wu TH, Lin CH, et al. **Can iterative reconstruction improve imaging quality for lower radiation CT perfusion? Initial experience.** *AJNR Am J Neuroradiol* 2013;34:1516–21
18. Manninen AL, Isokangas JM, Karttunen A, et al. **A comparison of radiation exposure between diagnostic CTA and DSA examinations of cerebral and cervicocerebral vessels.** *AJNR Am J Neuroradiol* 2012;33:2038–42
19. Siebert E, Bohner G, Dewey M, et al. **320-slice CT neuroimaging: initial clinical experience and image quality evaluation.** *Br J Radiol* 2009;82:561–70
20. Moskowitz SI, Davros WJ, Kelly ME, et al. **Cumulative radiation dose during hospitalization for aneurysmal subarachnoid hemorrhage.** *AJNR Am J Neuroradiol* 2010;31:1377–82
21. Vano E, Fernandez JM, Sanchez RM, et al. **Patient radiation dose management in the follow-up of potential skin injuries in neuroradiology.** *AJNR Am J Neuroradiol* 2013;34:277–82
22. Smit EJ, Vonken EJ, van Seeters T, et al. **Timing-invariant imaging of collateral vessels in acute ischemic stroke.** *Stroke* 2013;44:2194–99
23. Spetzler RF, Martin NA. **A proposed grading system for arteriovenous malformations.** *J Neurosurg* 1986;65:476–83
24. Cognard C, Gobin YP, Pierot L, et al. **Cerebral dural arteriovenous**

fistulas: clinical and angiographic correlation with a revised classification of venous drainage. *Radiology* 1995;194:671–80
25. Borden JA, Wu JK, Shucart WA. **A proposed classification for spinal and cranial dural arteriovenous fistulous malformations and implications for treatment.** *J Neurosurg* 1995;82:166–79
26. Wang H, Ye X, Gao X, et al. **The diagnosis of arteriovenous malformations by 4D-CTA: a clinical study.** *J Neuroradiol* 2014;41:117–23
27. Willems PW, Taeshineetanakul P, Schenk B, et al. **The use of 4D-CTA in the diagnostic work-up of brain arteriovenous malformations.** *Neuroradiology* 2012;54:123–31
28. Siebert E, Diekmann S, Masuhr F, et al. **Measurement of cerebral circulation times using dynamic whole-brain CT-angiography: feasibility and initial experience.** *Neurol Sci* 2012;33:741–47
29. Fujiwara H, Momoshima S, Akiyama T, et al. **Whole-brain CT digital subtraction angiography of cerebral dural arteriovenous fistula using 320-detector row CT.** *Neuroradiology* 2013;55:837–43
30. Brouwer PA, Bosman T, van Walderveen MA, et al. **Dynamic 320-section CT angiography in cranial arteriovenous shunting lesions.** *AJNR Am J Neuroradiol* 2010;31:767–70
31. Salomon EJ, Barfett J, Willems PWA, et al. **Dynamic CT angiography and CT perfusion employing a 320-detector row CT: protocol and current clinical applications.** *Klin Neuroradiol* 2009;19:187–96
32. Willems PW, Brouwer PA, Barfett JJ, et al. **Detection and classification of cranial dural arteriovenous fistulas using 4D-CT angiography: initial experience.** *AJNR Am J Neuroradiol* 2011;32:49–53
33. Beijer TR, van Dijk EJ, de Vries J, et al. **4D-CT angiography differentiating arteriovenous fistula subtypes.** *Clin Neurol Neurosurg* 2013; 115:1313–16
34. Yamaguchi S, Takeda M, Mitsuhara T, et al. **Application of 4D-CTA using 320-row area detector computed tomography on spinal arteriovenous fistulae: initial experience.** *Neurosurg Rev* 2013;36:289–96; discussion 296
35. Demchuk AM, Dowlatshahi D, Rodriguez-Luna D, et al. **Prediction of haematoma growth and outcome in patients with intracerebral haemorrhage using the CT-angiography spot sign (PREDICT): a prospective observational study.** *Lancet Neurol* 2012;11:307–14
36. Becker KJ, Baxter AB, Bybee HM, et al. **Extravasation of radiographic contrast is an independent predictor of death in primary intracerebral hemorrhage.** *Stroke* 1999;30:2025–32
37. Sun SJ, Gao PY, Sui BB, et al. **"Dynamic spot sign" on CT perfusion source images predicts haematoma expansion in acute intracerebral haemorrhage.** *Eur Radiol* 2013;23:1846–54
38. Frölich AM, Wolff SL, Psychogios MN, et al. **Time-resolved assessment of collateral flow using 4D CT angiography in large-vessel occlusion stroke.** *Eur Radiol* 2014;24:390–96
39. Riedel CH, Zimmermann P, Jensen-Kondering U, et al. **The importance of size: successful recanalization by intravenous thrombolysis in acute anterior stroke depends on thrombus length.** *Stroke* 2011;42:1775–77
40. Frölich AM, Schrader D, Klotz E, et al. **4D CT angiography more closely defines intracranial thrombus burden than single-phase CT angiography.** *AJNR Am J Neuroradiol* 2013;34:1908–13
41. Pillai JJ, Lanzieri CF, Trinidad SB, et al. **Initial angiographic appearance of intracranial vascular occlusions in acute stroke as a predictor of outcome of thrombolysis: initial experience.** *Radiology* 2001; 218:733–38
42. Suarez JI, Sunshine JL, Tarr R, et al. **Predictors of clinical improvement, angiographic recanalization, and intracranial hemorrhage after intra-arterial thrombolysis for acute ischemic stroke.** *Stroke* 1999;30:2094–100
43. Christoforidis GA, Mohammad Y, Avutu B, et al. **Arteriographic demonstration of slow antegrade opacification distal to a cerebrovascular thromboembolic occlusion site as a favorable indicator for intra-arterial thrombolysis.** *AJNR Am J Neuroradiol* 2006;27: 1528–31
44. Frölich AM, Psychogios MN, Klotz E, et al. **Antegrade flow across incomplete vessel occlusions can be distinguished from retrograde collateral flow using 4-dimensional computed tomographic angiography.** *Stroke* 2012;43:2974–79
45. Ringelstein EB, Biniek R, Weiller C, et al. **Type and extent of hemispheric brain infarctions and clinical outcome in early and delayed middle cerebral artery recanalization.** *Neurology* 1992;42:289–98
46. McVerry F, Liebeskind DS, Muir KW. **Systematic review of methods for assessing leptomeningeal collateral flow.** *AJNR Am J Neuroradiol* 2012;33:576–82
47. Miteff F, Levi CR, Bateman GA, et al. **The independent predictive utility of computed tomography angiographic collateral status in acute ischaemic stroke.** *Brain* 2009;132(pt 8):2231–38
48. Kucinski T, Koch C, Eckert B, et al. **Collateral circulation is an independent radiological predictor of outcome after thrombolysis in acute ischaemic stroke.** *Neuroradiology* 2003;45:11–18
49. Maas MB, Lev MH, Ay H, et al. **Collateral vessels on CT angiography predict outcome in acute ischemic stroke.** *Stroke* 2009;40:3001–05
50. Souza LC, Yoo AJ, Chaudhry ZA, et al. **Malignant CTA collateral profile is highly specific for large admission DWI infarct core and poor outcome in acute stroke.** *AJNR Am J Neuroradiol* 2012;33: 1331–36
51. Tan IY, Demchuk AM, Hopyan J, et al. **CT angiography clot burden score and collateral score: correlation with clinical and radiologic outcomes in acute middle cerebral artery infarct.** *AJNR Am J Neuroradiol* 2009;30:525–31
52. Orrison WW, Snyder KV, Hopkins LN, et al. **Whole-brain dynamic CT angiography and perfusion imaging.** *Clin Radiol* 2011;66:566–74
53. Menon BK, O'Brien B, Bivard A, et al. **Assessment of leptomeningeal collaterals using dynamic CT angiography in patients with acute ischemic stroke.** *J Cereb Blood Flow Metab* 2013;33:365–71
54. Oei M, Manniesing R, Meijer FJ, et al. **One-step-stroke imaging: does an interleaved acquisition of cerebral CT perfusion and CTA of the carotids affect CTP values.** In: *Proceedings of the European Congress of Radiology*, Vienna, Austria. March 6–10, 2014